AEC
RESEARCH
and
DEVELOPMENT
REPORT

BNWL-305
4

PHYSICS SURVEY CALCULATIONS FOR A PuO_2-UO_2 FUEL IN IDEALIZED H_2O POWER REACTORS

R. C. LIIKALA and U. P. JENQUIN

JULY, 1966

BATTELLE-NORTHWEST

BATTELLE MEMORIAL INSTITUTE / PACIFIC NORTHWEST LABORATORY

PACIFIC NORTHWEST LABORATORY
RICHLAND, WASHINGTON
operated by
BATTELLE MEMORIAL INSTITUTE
for the
UNITED STATES ATOMIC ENERGY COMMISSION UNDER CONTRACT AT(45-1)-1830

PRINTED BY/FOR THE U. S. ATOMIC ENERGY COMMISSION

AEC-RLOO RICHLAND, WASH.

BNWL-305
UC-80

PHYSICS SURVEY CALCULATIONS FOR A PuO_2-UO_2 FUEL IN IDEALIZED H_2O POWER REACTORS

By

R. C. Liikala and U. P. Jenquin

Reactor Lattice Physics Section
Reactor Physics Department

July, 1966

FIRST UNRESTRICTED DISTRIBUTION MADE NOV 2 '66

PACIFIC NORTHWEST LABORATORY
RICHLAND, WASHINGTON

Printed in USA. Price $2.00. Available from the
Clearinghouse for Federal Scientific and Technical Information
National Bureau of Standards
U.S. Department of Commerce
Springfield, Virginia

TABLE OF CONTENTS

Page No.

INTRODUCTION 1

FUEL LATTICE ARRANGEMENT AND REACTOR ENVIRONMENT 2

THEORETICAL METHODS 3

CALCULATIONAL RESULTS 3
    Moderator Heating 3
    Fuel Heating 8
    Moderator Voids 9
    Average Effects 13

FINITE SYSTEMS 13
    Effective Multiplications 13

CONCLUSIONS 15

REFERENCES 16

APPENDIX A 18

LIST OF FIGURES

Figure Page No.

1 Reactivity Variation with Moderator Temperature for Various Lattices 4

2 Reactivity as a Function of Moderator to Fuel Volume Ratio at Various Moderator Temperatures 5

3 Moderator Temperature Coefficients of Reactivity as a Function of Lattice Spacing 5

4 k_∞ as a Function of Hydrogen to Plutonium Atom Ratio 6

5 Reactivity Variation with Fuel Temperature for Various Lattices 9

6 Fuel Temperature Coefficients of Reactivity as a Function of Lattice Spacing 10

7 Reactivity Variation with Moderator Void Content for Various Lattices 10

8 Reactivity as a Function of Lattice Spacing at Various Void Fractions 11

9 Moderator Void Coefficients of Reactivity as a Function of Lattice Spacing 12

10 Average Reactivity Coefficients as a Function of Lattice Spacing 14

LIST OF TABLES

Table Page No.

I Calculational Temperature and Void Conditions 2

II Group Parameters at Various Moderator Temperatures 7

III Group Parameters at Various Moderator Void Contents 12

IV Calculated Values of L^2 and τ for Converting Infinite Multiplication k_∞ to Effective Multiplications k_{eff} 14

V Comparison of Effective Multiplications Using Multigroup Diffusion Theory (M.D.T.) Age-Diffusion Theory (A.D.T.) and Modified Age Diffusion Theory (M.A.D.T.) for some PuO_2-UO_2 Fueled-Critical Experiments 15

A-1 Dancoff Factors 18

PHYSICS SURVEY CALCULATIONS FOR A PuO_2-UO_2 FUEL IN IDEALIZED H_2O POWER REACTORS

INTRODUCTION

The interest in utilizing plutonium as a power reactor fuel is becoming widespread. The USAEC buyback guarantees for plutonium which are currently in effect will disappear in the near future.(1) Thus, the economics of competitive nuclear power will rest heavily on the degree to which plutonium is utilized in power reactors. Most indications are that plutonium is "best" utilized as a fast reactor fuel. However, the fast power reactor is yet in the developmental state and the commercial fast power reactor probably won't appear before the 1980's. In the interim, the possible uses of plutonium as a thermal reactor fuel are being investigated. Some information concerning the behavior of plutonium fuel in a heavy water (D_2O) reactor has been accumulated from the plutonium recycle program(2) utilizing the Plutonium Recycle Test Reactor (PRTR). A batch core experiment is scheduled to get underway in mid 1966 in the PRTR. This experiment(3), labelled the high power density core (HPDC), will consist of irradiating plutonium fuel (2w/oPuO_2-UO_2) to obtain experimental data relating excess reactivity and fuel composition as functions of time.

Over the past few years, clean critical and approach to critical experiments for a variety of plutonium fueled light water (H_2O) lattices have been performed,(4-7) at Pacific Northwest Laboratores and are continuing.(8) These experiments provide a foundation in establishing a sound technical basis for utilizing plutonium fuel in light water power reactors. Two power reactor experiments which include partial loadings of plutonium fuel have also begun.(9-12) The first experiment is a joint program between Pacific Northwest Laboratory and Argonne National Laboratory in which plutonium fuel will be irradiated in the Experimental Boiling Water Reactor (EBWR). The other power reactor experiment is the Saxton plutonium program(12), in which plutonium fuel will be irradiated in the Saxton reactor. The Saxton reactor is a pressurized H_2O system whereas the EBWR is a boiling H_2O system. Both programs seek to develop information on plutonium utilization in prototypes of commercial thermal power reactors. Thus, over the next few years, a considerable body of information will be accumulated concerning the behavior of plutonium fuel in H_2O power reactors. However, estimates of the physics behavior for plutonium fueled-H_2O power systems are currently needed. Because of the general lack of experimental information regarding the physics characteristics of plutonium fuel in H_2O power reactor environments, a calculational survey study has been carried out in an attempt to satisfy this need.

Our data are presented for a variety of conditions which were selected to cover the range of interest for both pressurized and boiling H_2O systems. We limit this portion of the investigation to the reactivity effects associated with changes in moderator and fuel temperature, and moderator void. The other portions of the investigation which entail describing the burnup behavior, temperature and void reactivity characteristics versus burnup and a comparison to "equivalent" UO_2 systems will be reported at a later date. For the sake of simplicity and generality we list results only for infinite systems. Also, the power reactor systems considered are idealized in the sense they are simple, clean systems and contain none of the complexities present in most power reactors (control rods, fuel element boxes, etc.). The infinite multiplications, k_∞'s are separated into parameters which describe the relative thermal and epithermal effects (i.e., components of k_∞). We also include data which can be utilized in converting any result for the infinite system (k_∞) to a finite system (k_{eff}).

FUEL LATTICE ARRANGEMENT AND REACTOR ENVIRONMENT

The "typical" plutonium fuel for a light water power reactor was selected as a mixture of plutonium oxide and uranium oxide. This type of fuel is being utilized in both the EBWR and Saxton plutonium experiments. The results of an economic optimization study(13) for light water power reactors indicate an optimum fuel contains near 2.75 wt% fissile material. Thus, the fuel selected as "typical" contains 2 wt% PuO_2 in UO_2, the uranium being natural. The Pu^{240} content in plutonium is assumed to be 8 wt%. The fuel dimensions selected are identical to the EBWR fuel. The fuel (PuO_2-UO_2) is 0.372 in. in diameter, is clad with 0.025 in. thick Zircoloy-2, and has a fuel density assumed at 88% of theoretical (i.e. 9.65 g/cm^3). Lattices which were thought to cover the range from undermoderated to overmoderated, for room temperature moderator were selected. The lattices are hexagonal with pin spacings of 0.55, 0.60, 0.70, and 0.80 in. respectively. These lattices are near identical geometrically to those of the EBWR fueled-H_2O critical experiments,(7) and are identical in fuel enrichment to critical experiments now being performed.(8) The conditions of moderator temperature, fuel temperature, and moderator void for the lattices are listed in Table I and were selected as being representative of power reactor environment.

TABLE 1. Calculational Temperature and Void Conditions

Condition	Calculational Points
Moderator Heating	20, 195, and 255 °C
Fuel Heating	20, 472, and 1020 °C
Moderator Voids	0, 15, and 30%

THEORETICAL METHODS

The theoretical methods employed are identical to those used in analysis of the plutonium fueled-H_2O critical experiments, and the experiments in the EBWR facility itself.(10) They consist of using the codes HRG(14), THERMOS(15), and TEMPEST(16) to obtain multigroup cell homogenized cross sections for use in a multiplication calculation.

The unit lattice cell is assumed to be made up of three cylindrical regions 1) fuel, 2) clad, and 3) moderator with reflecting cell boundary conditions. Thermal effects were computed using the THERMOS and TEMPEST codes and nonthermal effects computed using the HRG code. In computing resonance absorption, the effect of surrounding rods in the lattice must be accounted for, so the Dancoff-Ginsburg correction factors were utilized to account for this "so called" shadowing. The Dancoff factors C_i included the shadowing due to the 18 nearest fuel rods. The effects of clad in the Dancoff factors were neglected, and the values utilized in our computations are listed in Appendix A. The moderator scattering kernal was computed for each temperature by GAKER which is a subsidiary code to THERMOS and is based on the Nelkin model for H_2O[17]. All other thermal scatter-transfers within the cell (i.e., clad and fuel) were based on a gas model scattering kernel for the constituent materials (again at the material temperature). The cell averaged cross sections obtained from the THERMOS-HRG cell calculations are then used in an infinite multiplication calculation. These infinite multiplication factors are computed from the relationship,

$$k_\infty = \frac{\nu\overline{\Sigma}_{f1}\overline{\Phi}_1 + \nu\overline{\Sigma}_{f2}\,\overline{\Phi}_2}{\overline{\Sigma}_{a_1}\,\overline{\Phi}_1 + \overline{\Sigma}_{a_2}\,\overline{\Phi}_2} \qquad (1)$$

where subscripts 1 and 2 refer to nonthermal (10 MeV to 0.683 eV) and thermal (0.683 to 0.0 eV) energy groups of neutrons respectively. The non thermal to thermal flux normalization is $\overline{\Phi}_1\,\overline{\Sigma}_{out\ 1\rightarrow 2} = \overline{\Phi}_2\,\overline{\Sigma}_{a2}$, and substituting this normalization into equation (1) gives

$$k_\infty = \frac{\nu\overline{\Sigma}_{f1}\,(\overline{\Sigma}_{a2}/\overline{\Sigma}_{out\ 1\rightarrow 2}) + \nu\overline{\Sigma}_{f2}}{\overline{\Sigma}_{a1}\,(\overline{\Sigma}_{a2}/\overline{\Sigma}_{out\ 1\rightarrow 2}) + \overline{\Sigma}_{a2}} \qquad (2).$$

The TEMPEST code is utilized in computing only the thermal diffusion coefficients which can be utilized in computing effective multiplications, k_{eff} (i.e., converting from infinite to finite systems).

CALCULATIONAL RESULTS

MODERATOR HEATING

Values of the infinite multiplication factor were calculated for the moderator temperatures listed in Table I for all lattice spacings at a constant fuel temperature of 20 °C. The reactivity response to these moderator temperature changes is shown in Figure 1 for each lattice.

For the three smallest lattice spacings (0.55 through 0.70 in.) k_∞ decreases; thus, they represent undermoderated lattices.* Likewise, the 0.80 inch lattice is overmoderated

---

* *Undermoderated with respect to* k_∞ *not necessarily keff.*

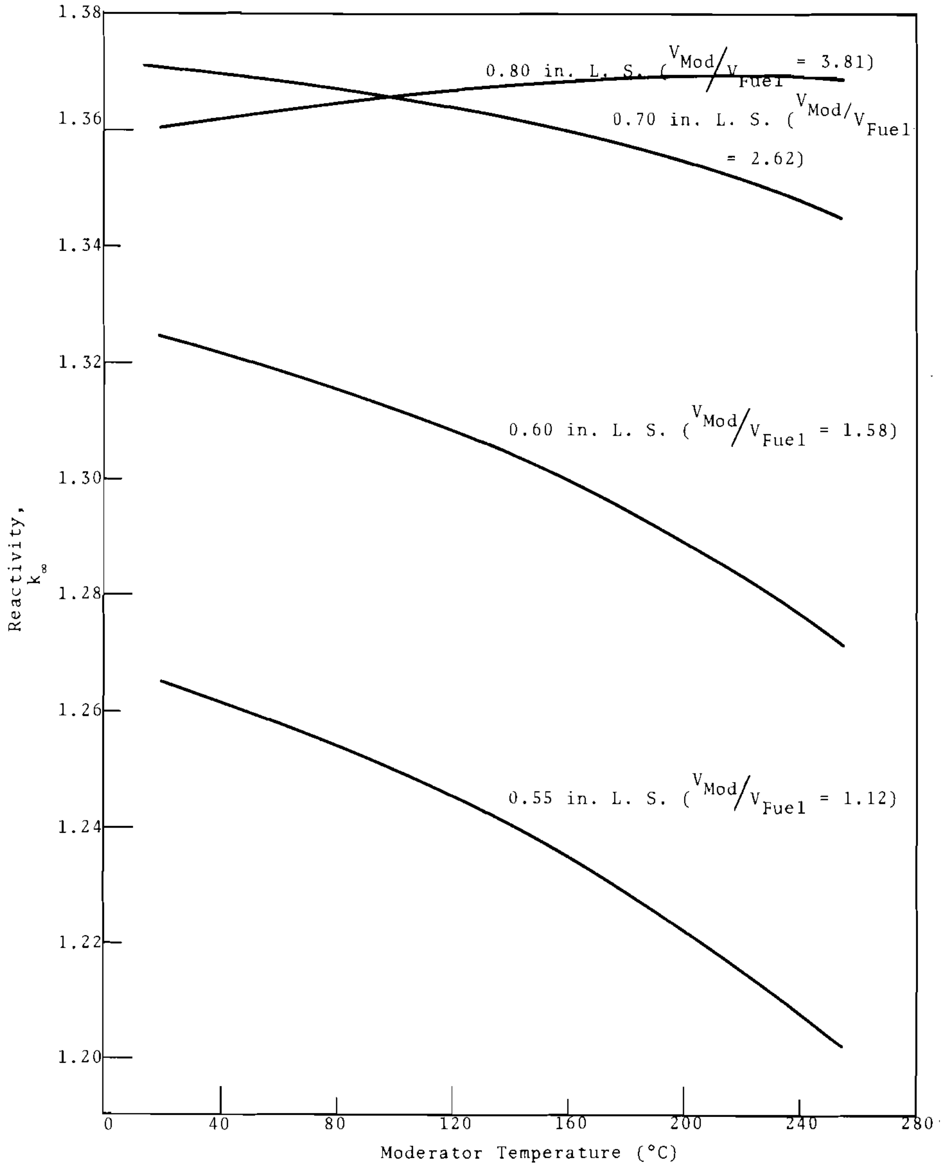

FIGURE 1. Reactivity Variation with Moderator Temperature for Various Lattices

since k_∞ increases with moderator temperature throughout the range of moderator temperatures. In Figure 2, the variation of k_∞ with moderator to fuel volume ratio is shown for each moderator temperature. Of important note is that a lattice with a moderator to fuel ratio of 3.3 "effectively" undergoes no change in k_∞ between 20 and 195 °C moderator temperatures; hence, an average null moderator temperature coefficient for this range of temperatures. At a moderator to fuel ratio of 3.6, k_∞ increases as the moderator heats to 195 °C, then decreases as the moderator temperature goes from 195 to 225 °C.

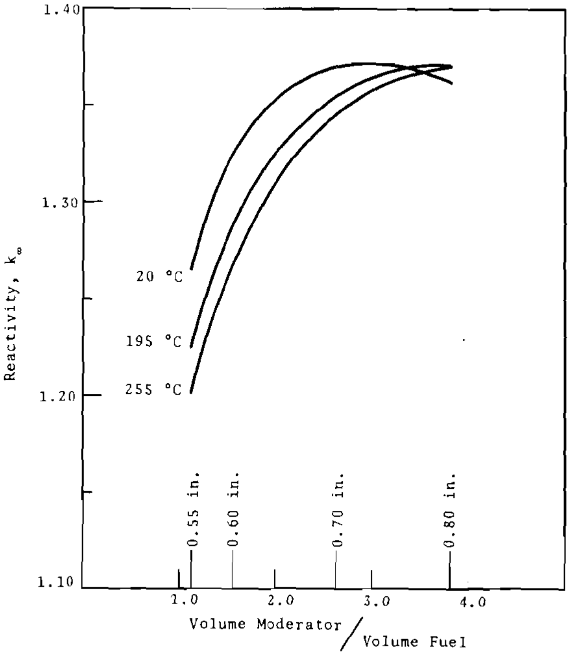

FIGURE 2. Reactivity as a Function of Moderator to Fuel Volume Ratio at Various Moderator Temperatures

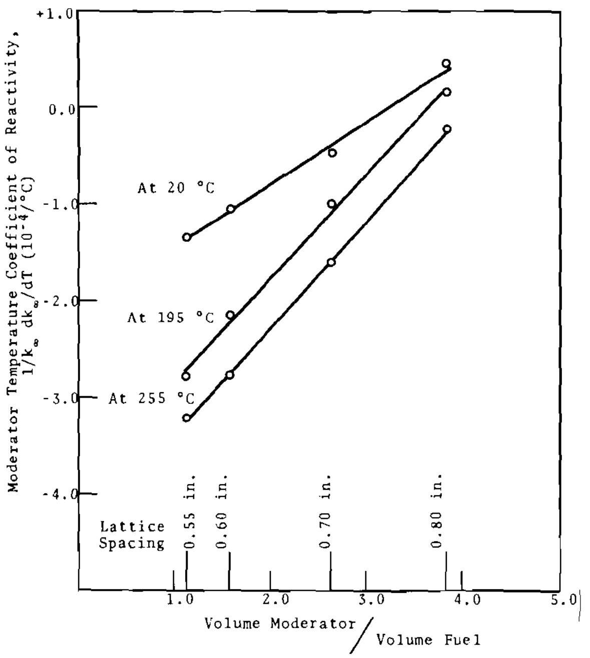

FIGURE 3. Moderator Temperature Coefficients of Reactivity as a Function of Lattice Spacing

Above a moderator to fuel ratio of 3.6, k_∞ increases for any increase in moderator temperature above 20 °C. Thus, moderator temperature coefficients for these lattices are not constant values, but rather depend strongly on the moderator temperature. This is better illustrated in Figure 3, where moderator temperature coefficients of reactivity at various temperatures are plotted as a function of lattice spacing. The moderator temperature coefficient at 20 °C is a factor of about 2.3 smaller than the value at 255 °C. To use a value for the moderator temperature coefficient determined for small temperature changes near 20 °C, for extrapolating to higher moderator temperatures could lead to large errors; the errors being largest at the close spaced lattices. The best fit (eyeball) straight line was drawn connecting the points in Figure 3.

An index frequently utilized in describing the reactivity variations to moderator temperature increases is the hydrogen to plutonium atom ratio (H/Pu). Moderator temperature changes are reflected by changes in H_2O density. By knowing the variation of k_∞ with lattice spacing for 20 °C moderator, a plot of k_∞ versus H/Pu atom ratio can be made. Thereupon any change in k_∞ due to moderator heating supposedly can be obtained directly from this curve. In utilizing the H/Pu ratio as an index, the spectral effect due to temperature dependence of thermal scattering kernel for H_2O is neglected. The discrepancy involved in this assumption is shown in Figure 4. With the 0.60 in. lattice as an example, the H/Pu ratio yields an expected value of k_∞ at 255 °C moderator temperature of 1.285. The calculated value at 255 °C is 1.272, as shown. Thus an

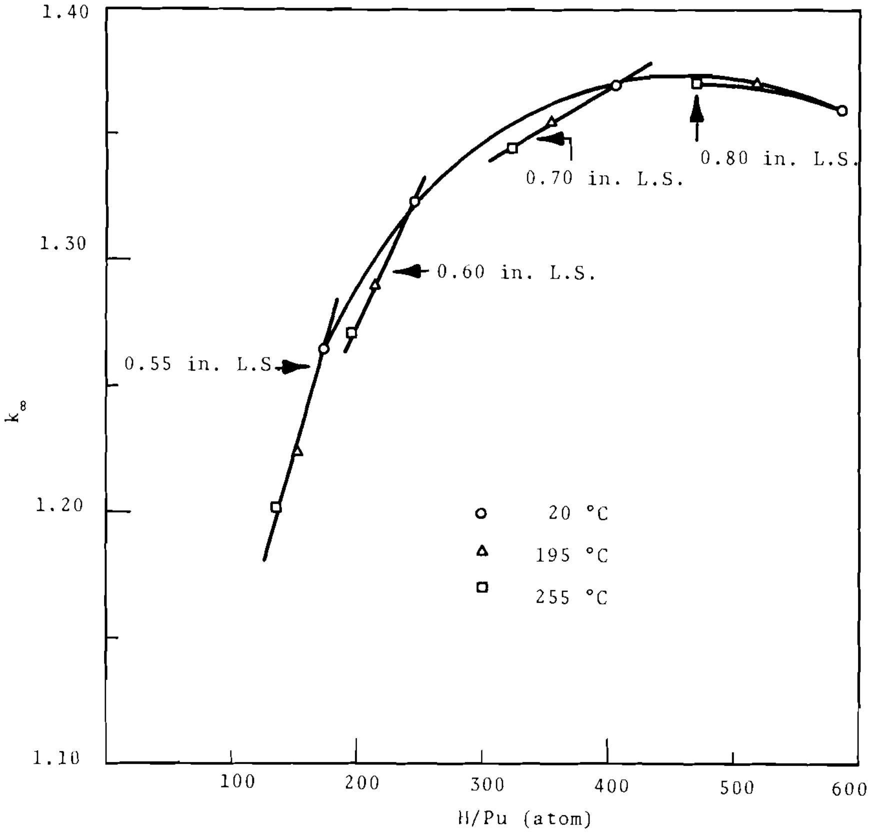

FIGURE 4. k_∞ as a Function of Hydrogen to Plutonium Atom Ratio

error of about 1% in k_∞ would result in determining k_∞ at 255°C moderator using the H/Pu ratio alone.

To determine what particular events (thermal or nonthermal) give rise to the k_∞ changes, we define some parameters to describe these thermal and nonthermal effects in k_∞. The thermal effects are lumped into three parameters—$\overline{\eta}f$, $\overline{\eta}$, and f—which are all obtained from the calculations using the THERMOS code. The ratio of the cell averaged thermal cross sections $\nu\overline{\Sigma}_{f_2}$ and $\overline{\Sigma}_{a_2}$ is denoted as $\overline{\eta}f$. The cell average value of $\overline{\eta}$ is the ratio of $(\nu\overline{\Sigma}_{f_2} \div \overline{\Sigma}_{a2})_{FUEL}$, and f is the usual thermal utilization, $\Sigma_{a_2\ FUEL} / \Sigma_{a_2}$ cell. To describe the relative resonance effects, resonance utilization factors, f_{ri}, defined as the ratio of cell averaged values of $\overline{\Sigma}ai$ to $\overline{\Sigma}ri$ are defined, where i refers to particular neutron energy groups and $\overline{\Sigma}r$ is the removal cross section (i.e., $\Sigma a + \Sigma out$). Two values of f_{ri} corresponding to an energy group from 1.17 x 10^4 to 2.38 eV and an energy group from 2.38 to 0.683 eV are given*. These values describe the relative changes due to U^{238} and Pu^{240} resonance absorption. The values of these parameters for each moderator temperature are shown in Table II.

---

* *Values obtained from the HRG cell calculations.*

We assume that events above the resonance region (i.e., fast effect) are not altered sufficiently as the reactor conditions change such that the above defined parameters can be used alone to account for the changes in k_∞.

Looking first at parameter changes as a function of lattice spacing for a constant temperature one can notice that as lattice spacing increases a) $\bar{\eta}f$ decreases, b) f_r decreases, and c) k_∞ increases, goes through a maximum, and then decreases. If the 0.55 to 0.70 inch lattices are undermoderated and the 0.80 inch lattice overmoderated, as defined then k_∞ follows the trend in f_r for the undermoderated lattices and follows the trend in $\bar{\eta}f$ for the overmoderated lattices. Thus, resonance absorption effects dominate in undermoderated lattices and thermal absorption effects dominate in overmoderated lattices for this fuel. The changes in $\bar{\eta}f$ as a function of lattice spacing at constant temperature follow the trend in f rather than $\bar{\eta}$.

An examination of the parameter changes for each lattice as a function of increasing moderator temperature points out that f_r decreases for all lattice spacings and that $\bar{\eta}f$ decreases for the 0.55 and 0.60 in. lattices and increases for the 0.70 and 0.80 in. lattices. The changes in $\bar{\eta}f$ as a function of temperature follow the trend

TABLE II. Group Parameters at Various Moderator Temperatures

Lattice spacing in.	Moderator Temperature °C	k_∞	$\bar{\eta}f_{thermal}$	$\bar{\eta}_{thermal}$	$f_{thermal}$	f_rU^{238}	f_rPu^{240}
0.55	20	1.265	1.675	1.752	0.956	0.298	0.117
	195	1.224	1.658	1.715	0.967	0.326	0.128
	255	1.202	1.657	1.707	0.970	0.347	0.136
H_2O Density (ρ_{H_2O}) at 255 °C,	Scattering kernel for H_2O* at 20 °C		1.684	1.745	0.964		
0.60	20	1.324	1.653	1.762	0.938	0.235	0.091
	195	1.290	1.643	1.721	0.954	0.258	0.101
	255	1.272	1.643	1.712	0.960	0.276	0.108
ρ_{H_2O} (255 °C), P(E, E') 20 °C			1.669	1.756	0.950		
0.70	20	1.370	1.591	1.776	0.896	0.160	0.062
	195	1.356	1.601	1.730	0.925	0.178	0.069
	255	1.345	1.608	1.720	0.935	0.191	0.075
ρ_{H_2O} (255 °C), P(E, E') 20 °C			1.625	1.720	0.918		
0.80	20	1.360	1.516	1.784	0.850	0.117	0.046
	195	1.370	1.547	1.737	0.891	0.131	0.052
	255	1.370	1.563	1.726	0.901	0.142	0.056
ρ_{H_2O} (255 °C), P(E, E') 20 °C			1.567	1.779	0.880		

* *Denoting the H_2O scattering kernel as P(E,E').*

in $\bar{\eta}$ for the 0.55 through 0.70 in. lattices and then follow the change in f for the 0.80 in. lattice. Thus, k_∞ as a function of temperature for an undermoderated lattice follows the change in $\bar{\eta}f$ and f_r since they both decrease. The 0.70 in. lattice results show that $\bar{\eta}f$ and k_∞ do not turn around simultaneously as a function of temperature; however, the lattice is undermoderated and f_r dominates. We also separate $\bar{\eta}f$ into an H_2O density effect and the temperature dependence of the scattering kernel effect. In the fourth row of Table II under each lattice spacing we list the results of a calculation whereby the H_2O density corresponds to 255 °C but the scattering kernel for H_2O is based on a 20 °C physical temperature. The results show that the density represents a positive contribution to $\bar{\eta}f$, therefore, the scattering kernel temperature must represent a negative contribution which is large enough to overcompensate the density effect. Thus, as was shown in Figure 4, the scattering kernel temperature represents a large perturbation in computing moderator temperature coefficients. If the temperature dependence of the moderator scattering kernel was neglected the calculated moderator temperature coefficients, shown in Figure 3, would be vastly different. For example, the 1% difference in k_∞ for the 0.60 in. lattice leads to a moderator temperature coefficient of reactivity which differs by about 30%. The difference gets larger for tighter lattices.

The resonance absorption due to Pu^{240} (f_r Pu^{240}) becomes more important the tighter the lattice becomes, as shown in column 8 of Table II, but does not represent much of a contribution to the moderator temperature coefficient of reactivity at these concentrations of Pu^{240}.

FUEL HEATING

Values of the infinite multiplication factor were calculated for fuel temperatures of 20, 472, and 1020 °C. The moderator temperature was held constant at 255 °C. In computing the reactivity effects due to fuel heating, we neglect the Doppler broadening of the low energy resonances (∿0.3 eV) for U^{235} and Pu^{239}. The reactivity response to these fuel temperature changes is shown in Figure 5 for each lattice. The tightest lattice (0.55 in.) has the largest reactivity loss with fuel temperature increase. This change in reactivity is totally a Doppler effect since the thermal parameters $\bar{\eta}$ and f did not change throughout the range of fuel temperatures. The only fuel temperature effect incorporated in our thermal calculation was to change the physical temperature in the scattering kernel calculation (gas model) for each fuel isotope. Thus, the temperature affect on scatter-transfers in the fuel (plutonium, uranium, and oxygen) does not lead to reactivity variations for these lattices.

The fuel temperature coefficients of reactivity are shown in Figure 6 as a function of lattice spacing for each fuel temperature. The fuel temperature coefficient of reactivity at 20 °C is shown to be about a factor of two larger than the coefficient at

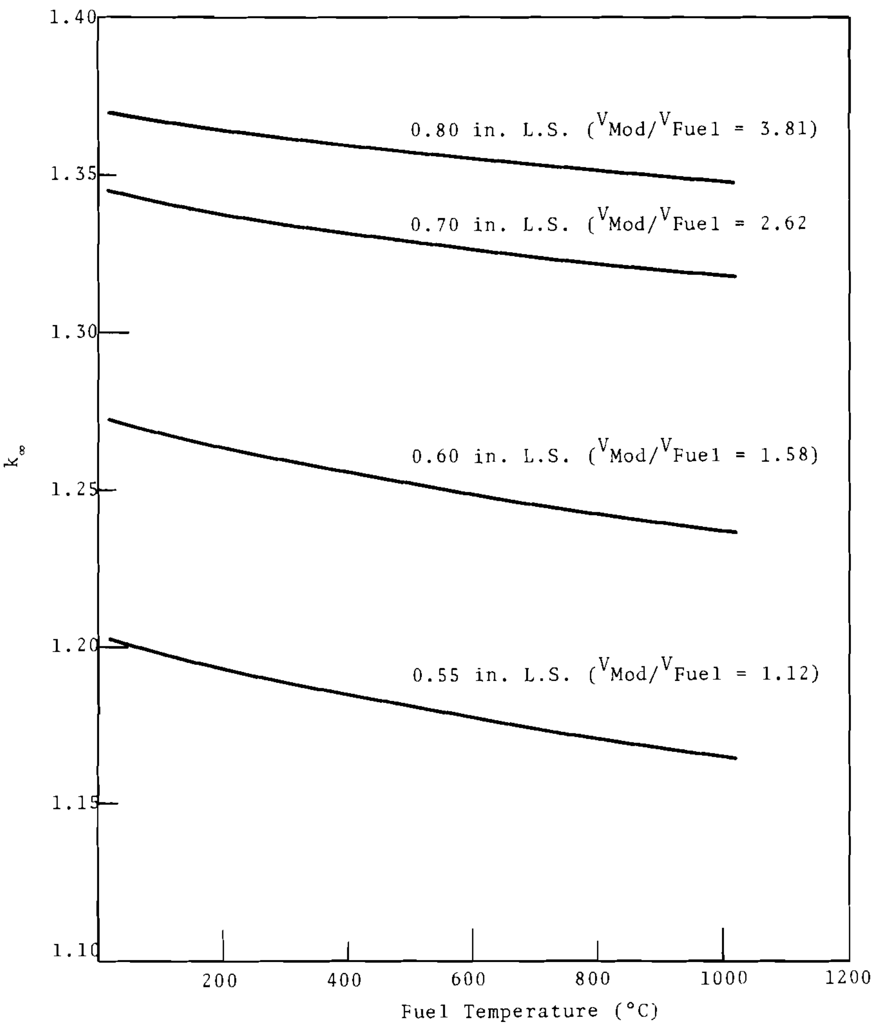

FIGURE 5. Reactivity Variation with Fuel Temperature for Various Lattices

1020 °C. Thus the fuel temperature coefficient of reactivity is non linear as a function of temperature as was the moderator temperature coefficient of reactivity.

The fraction of the total fuel temperature coefficient of reactivity due to resonance absorption in just U^{238} was determined by heating only the U^{238} in the fuel and computing a U^{238} Doppler coefficient of reactivity. The results show that approximately 82% of the fuel temperature coefficient of reactivity is due to U^{238}. This fraction is near constant as a function of fuel temperature but is slightly dependent on lattice in that it goes from ∿85% at the 0.55 in. lattice to ∿80% at the 0.80 in. lattice.

MODERATOR VOIDS

The results presented so far represent data for pressurized H_2O systems or interim conditions

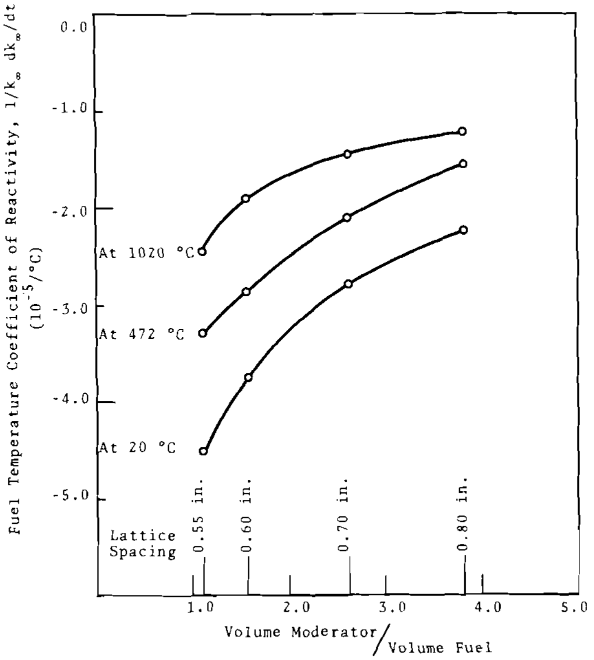

FIGURE 6. Fuel Temperature Coefficients of Reactivity as a Function of Lattice Spacing

for a boiling H_2O system. Infinite multiplications are now presented for boiling H_2O operating at a fuel temperature of 472 °C and a moderator temperature of 255 °C with moderator voids of 15% and 30%. Voids are defined as a uniform density change since no spatial void effects are included. Thus the reactivity effects due to void as quoted below represent, at best, gross estimates.

The calculated values of k_∞ versus void content for each lattice are shown in Figure 7. The tightest lattice exhibits the largest reactivity loss per void fraction. The variation in reactivity as a function of lattice spacing shown in Figure 8 for each void fraction and the moderator void coefficients of reactivity are shown

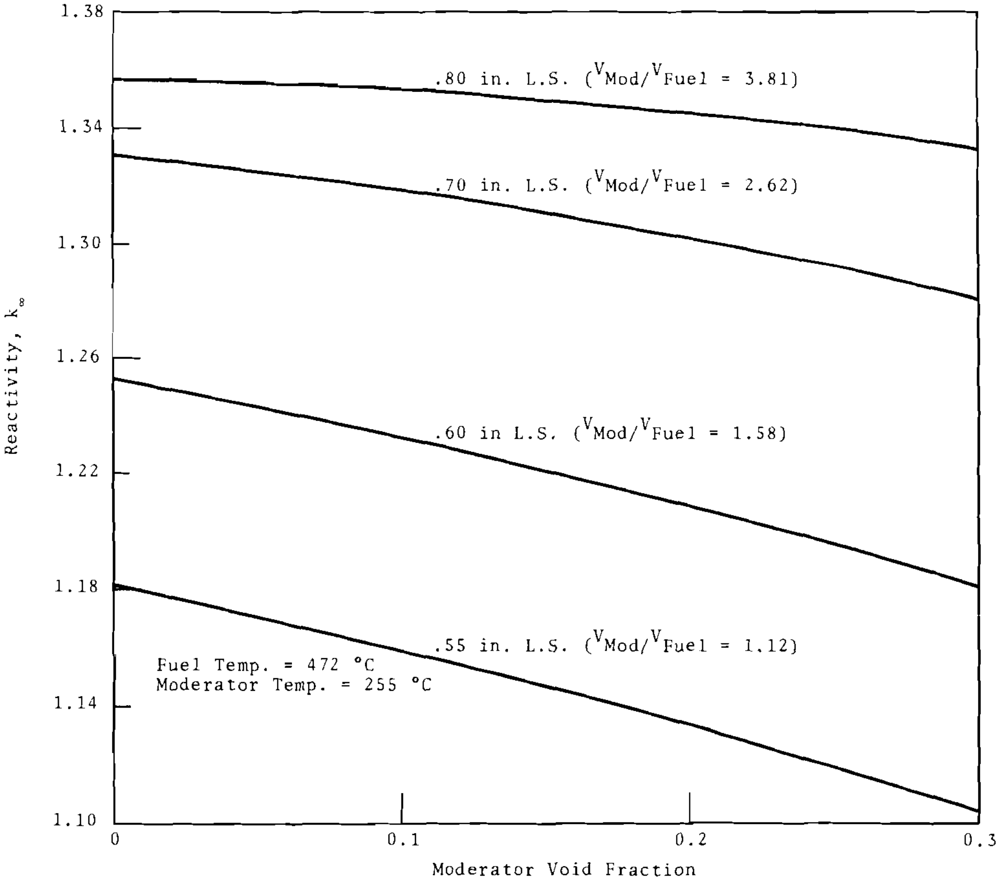

FIGURE 7. Reactivity Variation with Moderator Void Content for Various Lattices

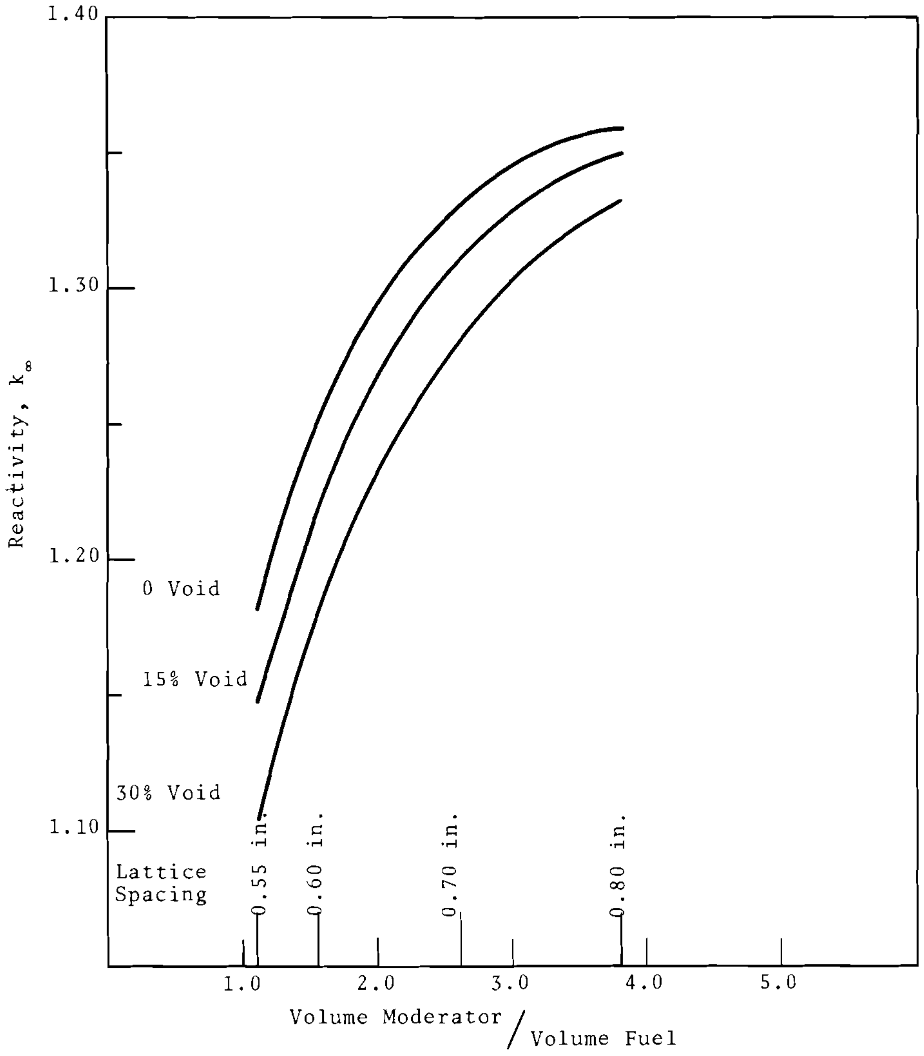

FIGURE 8. Reactivity as a Function of Lattice Spacing at Various Void Fractions

in Figure 9. As in the case of plotting moderator temperature coefficients of reactivity we have again drawn the best straight line between the points for the void coefficients.

The group parameters for each case of the void fraction investigation are listed in Table III. The negative void coefficients of reactivity result from an increase in resonance absorption with voiding, which is a large enough change to overcompensate for the increase in $\bar{\eta}f$. Since, by our terminology, all of these lattices are now undermoderated, the trend in k_∞ should follow the trends for undermoderated lattices as stated in the moderator heating section above, namely the change in the resonance escape probability. And just as is the case for moderator heating and undermoderated lattices, the change in $\bar{\eta}f$ results from a change in f. In comparing the $\bar{\eta}$ values for a given lattice with those

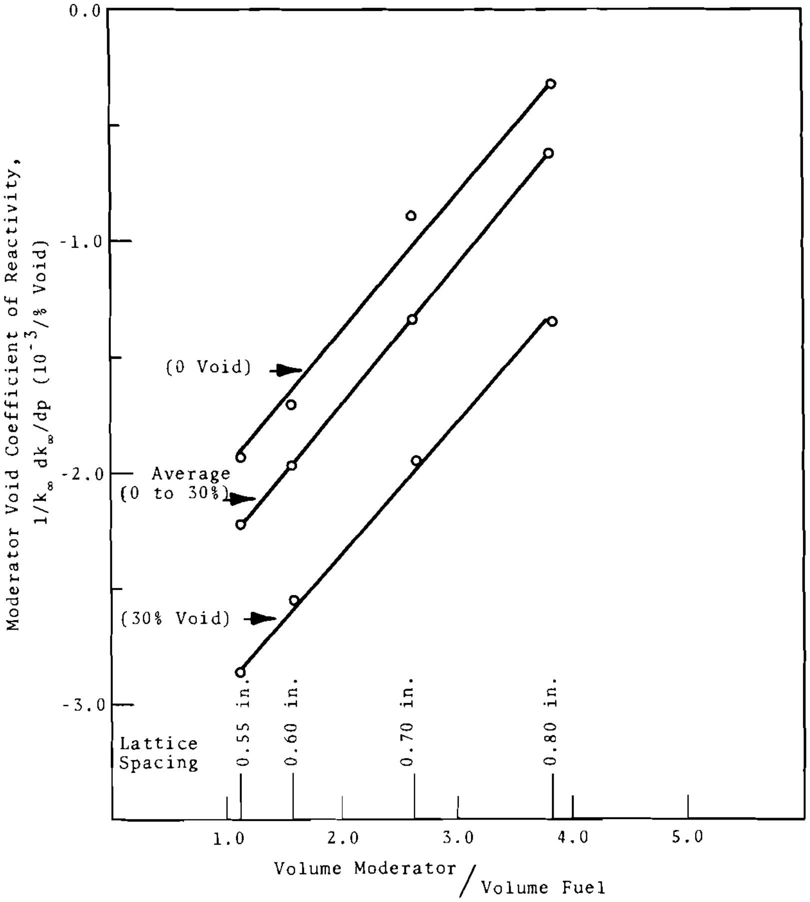

FIGURE 9. Moderator Void Coefficients of Reactivity as a Function of Lattice Spacing

TABLE III. Group Parameters at Various Moderator Void Contents

Lattice Spacing In.	Void Content %	k_∞	$\bar{\eta}f_{THERMAL}$	$\bar{\eta}_{THERMAL}$	$f_{THERMAL}$	$f_r^{U^{238}}$	$f_r^{fU^{240}}$
0.55	0	1.182	1.657	1.707	0.970	0.363	0.141
	15	1.147	1.661	1.705	0.974	0.400	0.156
	30	1.104	1.664	1.703	0.978	0.446	0.175
0.60	0	1.253	1.643	1.713	0.960	0.290	0.112
	15	1.221	1.651	1.710	0.965	0.323	0.125
	30	1.181	1.657	1.708	0.970	0.365	0.141
0.70	0	1.330	1.608	1.720	0.935	0.202	0.078
	15	1.310	1.622	1.718	0.944	0.228	0.088
	30	1.280	1.635	1.716	0.953	0.262	0.101
0.80	0	1.358	1.563	1.726	0.906	0.151	0.058
	15	1.350	1.584	1.724	0.919	0.171	0.066
	30	1.332	1.605	1.722	0.932	0.199	0.077

for the moderator heating case, one should note that whereas $\bar{\eta}$ decreased as the moderator heated, $\bar{\eta}$ remains constant as the moderator is voided. Thus, just as noted previously a moderator density change due either to heating or voiding (if we can truly represent voids as only a density change) does not change the thermal spectrum significantly (using $\bar{\eta}$ to represent thermal spectrum changes).

AVERAGE EFFECTS

As has been pointed out above, the temperature and moderator void coefficients depend quite strongly on the value of temperature and/or void. For purposes of estimating gross reactivity effects due to heating and voiding, average values of these reactivity coefficients are given in Figure 10. The averages are obtained by drawing a straight line between the end points of moderator temperature, fuel temperature, and void content for dk/dx, where x is either the temperature or void, and then dividing by the mean value of k_∞. The moderator temperature coefficient becomes positive for moderator-to-fuel volume ratios of 3.5. When estrapolated the void coefficient becomes positive near a moderator-to-fuel ratio of 4.8.

FINITE SYSTEMS

EFFECTIVE MULTIPLICATIONS

To convert the infinite multiplications, given above, to effective multiplications, k_{eff}, data is given in Table IV for use in the age-diffusion equation

$$k_{eff} = \frac{k_\infty e^{-B^2\tau}}{1+B^2L^2} \quad . \qquad (3)$$

Values of the diffusion area L^2 and the age τ along with all values of k_∞ are listed in Table IV. The diffusion area L^2 and τ are obtained from the cell average diffusion coefficients and removal cross section ($L^2 = \bar{D}/\bar{\Sigma}_a$ thermal, and $\tau = \bar{D}/\bar{\Sigma}_r$ nonthermal). The thermal diffusion coefficients were obtained from cell calculations using the TEMPEST code. Thus, for a given value of B^2, the results of these survey calculations for infinite systems can be converted to finite systems.

The degree of confidence in utilizing this simple scheme for conversion is now shown. Critical experiments(7) of 1.5 wt% PuO_2-UO_2 (EBWR fuel) in H_2O have been performed for a variety of lattices, three of which correspond directly to the lattice spacing utilized in this study. The size of the EBWR fuel rods used in the critical experiments are near identical to those of this study (i.e., same diameter fuel and clad thickness). However, the enrichment is 1.5 wt% PuO_2-UO_2 the uranium being depleted. Experiments(8) are currently being performed to determine critical masses of 2 wt% PuO_2-UO_2 (uranium natural) in H_2O, for 1/2 in. diameter fuel rods. Of these experiments we chose three lattices which cover the same range of moderator-to-fuel volume ratios as the lattices of this study. The results of effective multiplication calculations using multigroup diffusion therory in one space dimension; age-diffusion theory (Equa-

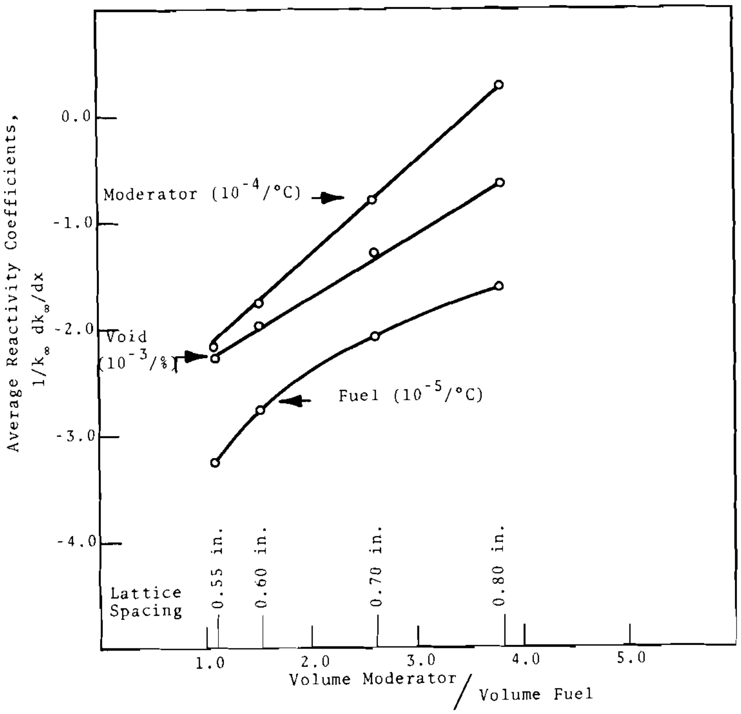

FIGURE 10. Average Reactivity Coefficients as a Function of Lattice Spacing

TABLE IV. Calculated Values of L^2 and τ For Converting Infinite Multiplication k_∞ to Effective Multiplications k_{eff}

	L.S. (in.)	k_∞	L^2 (cm^2)	τ^2 (cm^2)
Cold Fuel, Cold Mod.	0.55	1.265	1.30	35.21
	0.60	1.324	1.39	32.54
	0.70	1.370	1.61	29.76
	0.80	1.360	1.87	28.37
Cold Fuel, 195 °C Mod.	0.55	1.224	1.50	41.27
	0.60	1.290	1.64	38.81
	0.70	1.356	1.92	36.37
	0.80	1.370	2.28	35.24
Cold Fuel, 255 °C Mod.	0.55	1.202	1.70	46.02
	0.60	1.272	1.81	43.82
	0.70	1.345	2.14	41.79
	0.80	1.369	2.54	40.98
472 °C Fuel, 255 °C Mod., 0 V.F.	0.55	1.182	1.70	45.83
	0.60	1.253	1.80	43.68
	0.70	1.330	2.13	41.71
	0.80	1.358	2.54	40.93
1020 °C Fuel, 255°C Mod. 0 V.F.	0.55	1.164	1.70	45.72
	0.60	1.237	1.80	43.60
	0.70	1.318	2.13	41.66
	0.80	1.348	2.54	40.89
472 °C Fuel, 255 °C Mod., .15 V.F.	0.55	1.147	2.00	54.50
	0.60	1.221	2.12	53.02
	0.70	1.310	2.54	52.18
	0.80	1.350	3.03	52.27
472 °C Fuel, 255 °C Mod., .3 V.F.	0.55	1.104	2.30	66.17
	0.60	1.181	2.55	65.98
	0.70	1.280	3.12	67.34
	0.80	1.332	3.76	69.23

tion 3);and modified age-diffusion theory which results from the expansion of $e^{-B^2\tau}$* and combining into a migration area $M^2 = L^2 + \tau$. The multigroup diffusion theory calculation (4 groups of neutrons) assumed a two region reactor (homogeneous core + H_2O reflector with axial leakage accounted for by using

---

*

$$k_{eff} = \frac{k_\infty e^{-B^2\tau}}{1+B^2L^2}$$

$$= \frac{k_\infty}{(1 + B^2L^2)(1 + B^2\tau)}$$

$$\frac{k_\infty}{1 + B^2M^2}$$

where terms of the order B^4 are dropped.

transverse bucklings. Values of L^2 and τ for these lattices were again computed from the cell averaged values of D (diffusion coefficient) and Σ_r (removal cross section). In computing k_{eff} by using Equation (3) or the modified age-diffusion equation (i.e. $M^2 = L^2 + \tau$), experimental values of buckling Bg^2 were used. The calculated results are shown in Table V. The largest discrepancy from experiment occurs when the modified age-diffusion equation is utilized in computing k_{eff}. The difference between k_{eff}'s computed by using the age-diffusion equation (3) relative to the modified age-diffusion equation results from dropping terms in Bg^n for $n > 2$ in the expansion from the former Age Diffusion Theory to the latter Modified Age Diffusion Theory. Since the 2 wt% PuO_2-UO_2 criticals are smaller systems than the EBWR criticals, there is more leakage and discrepancies get larger. The k_{eff}'s calculated using the age-diffusion equation (3) are seen to be ∿1% different from those obtained using one dimensional diffusion theory.

CONCLUSIONS

Calculational results describing the physics behavior of a plutonium fuel in a power reactor which is light water cooled and moderated is presented as a survey study. A variety of fuel and moderator temperature conditions, as well as moderator void conditions, were selected to cover the range of interest for both pressurized and boiling light water systems. The data are presented for reactor systems which are

TABLE V. Comparison of Effective Multiplications Using Multigroup Diffusion Theory (M.D.T.) Age-Diffusion Theory (A.D.T.) and Modified Age Diffusion Theory (M.A.D.T.) for some PuO_2-UO_2 Fueled-Critical Experiments

k_{eff}-experiment = 1.000

EBWR FUEL (1.5 wt% PuO_2-UO_2)(3/8 in. Diam, 48 1/2 in. long)

	CALCULATED VALUES						
					k_{eff}		
Lattice Pitch (In.)	V_{Mod}/V_{Fuel}	k_∞	L^2 (cm^2)	τ (cm^2)	M.D.T.	A.D.T.	M.A.D.T.
0.55	1.099	1.195	1.77	38.61	1.000	0.993	1.008
0.60	1.557	1.248	1.84	35.75	0.998	0.988	1.012
0.71	2.705	1.275	2.08	32.40	0.999	0.988	1.016
0.80	3.788	1.249	2.35	31.10	0.997	0.989	1.013

(2 wt% PuO_2-UO_2)(1/2 in. Diam, 36 in. long)

	CALCULATED VALUES						
					k_{eff}		
Lattice Pitch (In.)	V_{Mod}/V_{Fuel}	k_∞	L^2 (cm^2)	τ (cm^2)	M.D.T.	A.D.T.	M.A.D.T.
0.80	1.489	1.338	1.40	32.92	0.998	0.993	1.031
0.93	2.452	1.407	1.63	30.04	0.998	0.996	1.040
1.143	4.345	1.327	2.15	28.00	0.994	0.997	1.031

infinite in size, however, the parameters necessary to convert the results to a finite size system are also given.

It is shown that the average reactivity coefficients are

- negative for all but the loose lattice for the moderator temperatures considered
- negative for all fuel temperatures
- and negative for all void fractions.

The overall temperature coefficient (moderator + fuel) is negative for all moderator to fuel ratios considered.

To accurately compute the moderator temperature coefficient of reactivity it is necessary to include the temperature dependence of the moderator scattering kernel. The calculational results for moderator temperature changes show that the changes in reactivity follow the trend of changes in resonance absorption for undermoderated systems* whereas the changes in reactivity follow the trend of changes in $\bar{\eta}f_{\text{thermal}}$ for overmoderated systems.

The fuel temperature coefficient of reactivity as calculated, is totally a Doppler effect. The Pu^{240} in plutonium contributes approximately 20% to this coefficient. For systems containing more Pu^{240} in plutonium than 8 wt%, the fractional contribution of Pu^{240} to the fuel temperature coefficient would be larger.

The reactivity variation with moderator void content is shown to follow the variation in resonance absorption.

The comparison of computed effective multiplications, using the Gaussian slowing down model (Equation 3), to experimental values indicates that the data given in Table IV can be used with fair success in estimating critical masses for any of the conditions listed.

REFERENCES

1. *Plutonium As a Power Reactor Fuel, Hw-75007, compiled by F. G. Dawson, Proceedings of American Nuclear Society Topical Meeting, Richland, Washington, September 13 and 14, 1962.*
2. *L. C. Schmid, Survey of Work at Hanford Laboratories in D_2O Moderated Systems, HW-SA-3456.*
3. *J. R. Worden, W. L. Purcell, and L. C. Schmid, Physics Experiment-High Power Density Core of the PRTR, BNWL-221, January 1966.*
4. *W. P. Stinson and L. C. Schmid, "Subcritical Measurements with 1.8 wt% Pu-@1 Rods in Light Water," Physics Research Quarterly Report, April, May, June, 1962, HW-74190, pp. 17-24. Juley 16, 1962.*
5. *W. P. Stinson, J. A. Marks, and L. C. Schmid, "Subcritical Measurements with 2.0 wt% Pu-Al Rods in Light Water," Physics Research Quarterly Report, July, August, September, 1963, HW-79054, pp. 43-46. October 15, 1963.*
6. *V. I. Neeley, R. C. Lloyd, and E. D. Clayton. "Neutron Multiplication Measurement with Pu-Al Alloy Rods in Light Water," HW-70944. August 29, 1961.*
7. *L. C. Schmid, R. C. Liikala, W. P. Stinson, and J. R. Worden. "Critical Masses and Bucklings of PuO_2-UO_2-H_2O Systems," Physics Research Quarterly Report, April, May, June, 1964, HW-83187, pp. 4-6, July 15, 1964. Also Trans. Am. Nuc. Soc. Vol. 7, No. 2. (1964).*
8. *R. C. Liikala and W. P. Stinson. "Experimental and Analytical Results for PuO_2-UO_2-H_2O Lattices," Trans. Am. Nuc. Soc. Vol. 9, No. 1. (1966)*

---

* *As we define overmoderated and undermoderated (see page 3)*

9. B. J. Toppel, et. al., Safety Analysis Associated With the Plutonium Recycle Experiment in EBWR, ANL-6841, November 1964, also, Some Physics Aspects of the Plutonium Experiment in EBWR, ANL-7019. April 1965.

10. R. C. Liikala, U. P. Jenquin, and W. A. Reardon, The PuO_2-UO_2 Experiment in the EBWR, BNWL-126, June 1965.

11. B. J. Toppel and R. Avery, Some Physics Aspects of the Plutonium Experiment in EBWR, ANL-7019, April 1965.

12. N. R. Nelson et. al., Saxton Plutonium Program Quarter Progress Reports, WCAP-3385-1 through 5.

13. Three Reactor Plutonium Optimization Study, (by Programming Staff), HW-77082 RD, (March 14, 1963).

14. J. L. Carter, Jr., HRG-Hanford Revised Gam (unpublished data).

15. H. C. Honeck, Jr. THERMOS, A Thermalization Transport Theory Code for Reactor Lattice Calculations, BNL-5826 (1961).

16. R. H. Shudde and J. Dyer, NAA Program Description, "TEMPEST - A Neutron Thermalization Code." North American Aviation Corportation, (1960).

17. M. Nelkin "Scattering of Slow Neutrons by Water," Phys. Rev., vol. 119, pp. 741-746. 1960.

18. J. R. Lilley, "Computer Code HFN-Multigroup Multiregion Neutron Diffusion Theory in One Space Dimension," HW-71545. November 17, 1961.

19. "Reactor Physics Constants", ANL-5800 Second Edition pp. 279-291, July 1963.

APPENDIX A

The Dancoff factors, C_i, were all obtained from tables published in ANL-5800, Second Edition.(18) A value of $\overline{\Sigma}_{\text{TOTAL}}^{\text{epithermal}}$ for full density H_2O was taken as 1.49 cm^{-1}. The values of $\overline{\ell}$ used as input to the HRG code were then computed by

$$\overline{\ell} = \frac{2r}{(1-C)} \qquad \text{(A-1)}$$

where r is the fuel radius and C is the Dancoff factor. The value of (1-C) is obtained from

$$(1-C) = (1-C_1)^6\ (1-C_2)^6\ (1-C_3)^6 \qquad \text{(A-2)}$$

where C_1 is the Dancoff factor for the 6 nearest rods,

C_2 is the Dancoff factor for the next 6 nearest rods, and

C_3 is the Dancoff factor for the next 6 nearest rods. Thus, a total of 18 rods are in the shadowing correction term. The values of C_1, C_2, and C_3 are listed in Table A-I.

TABLE A-I. Dancoff Factors

20 °C

L. S. (in.)	C_1	C_2	C_3	$\overline{\ell}$
0.55	0.0394	0.0038	0.0018	1.248
0.60	0.0285	0.0024	0.0009	1.146
0.70	0.0155	0.0009	0.0004	1.046
0.80	0.0088	0.0004	0.0001	0.999

195 °C

L. S. (in.)	C_1	C_2	C_3	$\overline{\ell}$
0.55	0.0444	0.0052	0.0026	1.300
0.60	0.0335	0.0034	0.0015	1.194
0.70	0.0189	0.0015	0.0007	1.074
0.80	0.0112	0.0007	0.0002	1.016

255 °C, 0 Void Fraction

L. S. (in.)	C_1	C_2	C_3	$\overline{\ell}$
0.55	0.0483	0.0064	0.0034	1.349
0.60	0.0375	0.0044	0.0022	1.237
0.70	0.0218	0.0021	0.0009	1.098
0.80	0.0133	0.0009	0.0004	1.032

255 °C, 0.15 Void Fraction

L. S. (in.)	C_1	C_2	C_3	$\overline{\ell}$
0.55	0.0545	0.0091	0.0050	1.440
0.60	0.0419	0.0064	0.0033	1.295
0.70	0.0269	0.0033	0.0015	1.145
0.80	0.0168	0.0015	0.0006	1.059

255 °C, 0.3 Void Fraction

L. S. (in.)	C_1	C_2	C_3	$\overline{\ell}$
0.55	0.0616	0.0123	0.0071	1.555
0.60	0.0490	0.0090	0.0048	1.388
0.70	0.0324	0.0047	0.0022	1.200
0.80	0.0219	0.0023	0.0007	1.099

DISTRIBUTION

Number of Copies	
1	A. B. Atomenergi P. O. Box 9042 Stockholm-9, Sweden Attn: B. Perohagen
2	Argonne National Laboratory Attn: Robert Avery B. Toppel
2	Atomic Energy Commission Division of Reactor Development and Technology Reactor Physics Branch Attn: I. F. Zartman
3	Atomic Energy Commission Division of Reactor Development and Technology Water Reactors Branch Attn: W. R. Voigt, Chief R. M. Grube (2)
1	Atomic Energy Commission Reactor Evaluation Staff Attn: J. M. Vallance
1	Atomic Energy Commission Division of Production Attn: F. P. Baranowski
2	Babcock and Wilcox Co. Lynchburg, Va. Attn: M. C. Edlund Donald Roy
1	Belgonucleaire 35 Rue Des Colonies Brussels, Belgium Attn: E. Fossoul
280	Division of Technical Information Extension Oak Ridge, Tennessee
4	Douglas United Nuclear Inc. Richland, Washington Attn: T. W. Ambrose R. Nilson C. E. Bowers G. F. Owsley
1	European Atomic Energy Community 51-53 Rue Belliard (EURATOM) Brussels 4, Belgium Attn: Pierre Kruys
1	General Atomic San Diego, California Attn: H. B. Stewart
3	General Electric Company Pleasanton, California Attn: L. P. Bupp E. A. Evans J. G. Carver
2	General Electric Company Richland, Washington Attn: M. C. Leverett W. S. Nechodom
4	General Electric Company San Jose, California Attn: S. Levy E. L. Zebroski D. L. Fischer R. Kanne
6	Richland Operations Office Richland, Washington Attn: P. G. Holsted H. A. Fouse W. E. Fry L. R. Lucas R. K. Sharp Technical Information Library
1	Savannah River Laboratory Aiken, South Carolina Attn: E. J. Hennelly
2	United Kingdom Atomic Energy Authority Atomic Energy Establishment Winfrith, Dorchester, Dorset, England Attn: C. G. Campbell G. H. Kinchin
2	United Nuclear Corporation White Plains, N. Y. Attn: G. A. Sofer J. R. Tomonto
4	Westinghouse Electric Corporation Pittsburgh, Pa. Attn: N. R. Nelson H. W. Graves F. L. Langford L. Orr

Number of Copies

114 Battelle-Northwest Laboratories
Richland, Washington

F. W. Albaugh
D. G. Albertson
C. L. Bennett
R. A. Bennett
S. R. Bierman
C. L. Brown
W. W. Brown
S. H. Bush
G. J. Busselman
J. J. Cadwell
J. L. Carter
D. E. Christensen
R. G. Clark
E. D. Clayton
G. M. Dalen
L. C. Davenport
F. G. Dawson
D. R. de Halas
B. H. Duane
E. A. Eschbach
S. L. Fawcett
J. R. Fishbaugher
D. G. Foster
H. A. Fowler
A. G. Gibbs
D. W. Glasgow
V. W. Gustafson
C. E. Haines
R. W. Hardie
O. K. Harling
R. A. Harris
H. Harty
C. M. Heeb
R. E. Heineman
H. L. Henry
N. A. Hill
P. L. Hofmann
R. H. Holeman
R. M. Humes
U. P. Jenquin (10)
R. L. Junkins
E. L. Kelly, Jr.
D. A. Kottwitz
J. W. Kutcher
D. D. Lanning
J. H. Lauby
B. R. Leonard, Jr.
W. R. Lewis
R. C. Liikala (15)
C. W. Lindenmeier
W. W. Little
R. C. Lloyd
L. L. Maas
D. R. Marr
R. P. Matsen
D. D. Matsumoto
R. E. Nightingale
L. J. Page
R. S. Paul
R. E. Peterson
W. W. Porath
W. A. Reardon
J. J. Regimbal
C. R. Richey
R. E. Schenter
J. E. Schlosser
L. C. Schmid
D. R. Skeen
J. D. Smith
R. B. Smith
R. I. Smith
K. B. Stewart
W. P. Stinson
J. J. Stoffels
D. H. Thomsen
V. O. Uotinen
M. T. Walling, Jr.
J. D. White
L. D. Williams
J. R. Worden
H. S. Zwibel
Technical Information Files (5)
Technical Publications (2)